Effect of Cerium Addition to a Hydrothermal Treatment on the Corrosion Protection of the Tartaric-Sulfuric Acid Anodized AA2524-T3

*Maysa Terada,[‡,***] Fernanda M. Queiroz,[*****] Helen Costenaro,[**] Victor H. Ayusso,[*] Marjorie Olivier,[****] Isolda Costa,[*] and Hercílio G. de Melo[**]*

To protect Al alloys from corrosion, standard procedures in the aerospace industry use chromium-based acid anodizing with subsequent post-treatment steps also containing hexavalent chromium (Cr(VI)) ions. However, environmental and health related concerns associated with Cr(VI) have encouraged the search for new surface treatments providing effective corrosion protection without the drawback of generating toxic residues. In this investigation, a hydrothermal treatment in aqueous solution with cerium ions is proposed as a post-treatment for tartaric-sulfuric acid (TSA) anodizing, and its effects on the AA2524-T3 alloy corrosion resistance investigated. The effect of Ce on the characteristics of the surface film formed, such as morphology and corrosion resistance, is investigated by scanning electron microscopy and electrochemical impedance spectroscopy (EIS). The results show that the hydrothermal treatment in solution containing Ce(III) ions presents a less stable behavior than the treatment in boiling water. However, the results of the EIS experiments show recovery of the protective properties of the system, indicating that some self-healing properties must be imparted to the system.

KEY WORDS: AA2524-T3, Ce(III) ions, tartaric-sulfuric acid (TSA)

INTRODUCTION

Chromium-based acid anodizing is one of the standard procedures used to protect aluminum alloys from corrosion in the aerospace industry.[1] The produced anodic layer exhibits the required corrosion resistance due to its self-healing properties.[2-4] Also, sealing processes with hexavalent chromium are used as an additional protection for materials used with organic coatings, as they promote not only adhesion of the coatings but also improve the corrosion resistance. The metallic oxide formed on the surface is homogeneous and insoluble, formed by trivalent and hexavalent chromium. However, this method of protection causes large environmental and health related problems due to the toxic residues generated, mainly hexavalent chromium compounds.[3-4] Moreover, the European regulation REACH (Registration, Evaluation, Authorization and Restriction of Chemicals) has planned the complete prohibition of hexavalent chromium in this industry since 2017.[5]

Recent studies recommend tartaric-sulfuric acid (TSA) anodizing, a chromium-free process, as a viable alternative.[6] It is environmentally compliant and provides corrosion resistance properties compatible with the requirements of the aerospace industry with appropriate paint adhesion.[7-8] In addition, it has been shown that it can produce oxide layers with corrosion resistance comparable to those formed in chromic acid baths.[6]

Depending on their application, anodized alloys need to be sealed to prevent aggressive species to reach the base metal.[6,9-10] López, et al.,[11] studied the sealing of an anodized layer on commercial pure aluminum using scanning electron microscopy (SEM), transmission electron microscopy (TEM), and electrochemical impedance spectroscopy (EIS) and proposed a detailed sealing mechanism for the porous anodized layer. According to the authors, initially, the pores are filled with water (sealing solution) and pore mouths are plugged by a top surface layer of acicular pseudoboehmite crystals and a compact intermediate layer. Below this latter layer, the pore is occupied by an aluminum hydroxide gel. In a second step, partial dissolution of the pore walls can be detected, increasing the pore diameter by 50% to 60%. This phenomenon starts during the sealing process and may continue for a long period upon exposure to mildly aggressive environments. Boehmite gel is present within the pores. Finally, the gel inside the pores is saturated by the progressive dissolution of the pore walls and precipitate as bayerite, $Al_2O_3{\cdot}3H_2O$, which is stable at ambient temperature, plugging the entire length of the pores. However, the sealing time (even when performed industrially) is too short to completely saturate the pores with bayerite, and sealing is completed during exposure of the sealed layer to mildly aggressive environments, like atmosphere.[11] This would explain the increased impedance often verified when aluminum anodized layers exposed for extended periods to the atmosphere are tested.[11-12] The sealing process is frequently performed in

Submitted for publication: October 3, 2018. Revised and accepted: June 19, 2019. Preprint available online: June 20, 2019, https://doi.org/10.5006/3063.
‡ Corresponding author. E-mail: maysaterada@uol.com.br.
* Nuclear and Energy Research Institute, Av. Prof. Lineu Prestes, 2242, CEP 05508-000, São Paulo, SP, Brazil.
** Polytechnic School of the University of São Paulo, Av. Prof. Mello de Moraes, 2463, 05508-030, São Paulo-SP, Brazil.
*** Escola e Faculdade de Tecnologia SENAI Suiço-Brasileira "Paulo E. Tolle", Rua Bento Branco de Andrade Filho, 379, 04757-000, São Paulo-SP, Brazil.
**** Faculty of Engineering, University of Mons, 20, Place du Parc, Mons, Belgium.

ISSN 0010-9312 (print), 1938-159X (online) © 2019 NACE International. Reproduction or redistribution of this article in any form is prohibited without express permission from the publisher.

boiling water[13] or in hexavalent chromium-containing solution.[9-10] The corrosion protection of sealed aluminum alloys in chromium-free solutions and the potential for replacement of chromating treatments is under evaluation based on their environmentally-friendly properties.[14] Inoue, et al., studied the incorporation of cerium ions into the surface layer formed by hydrothermal treatments on the AA2524 (UNS A92524[(1)]).[15]

For replacement of sealing treatments with hexavalent chromium-based additives, surface treatments with cerium ions have been studied. The literature reports several works with cerium as the most promising element to replace chromium in baths due to its self-healing properties.[16-18] Cerium compounds precipitate coherent oxide films on metal substrates, acting as cathodic inhibitors.[19-20] The literature also reports that post-treatments of 2 min or 5 min maintain the pores of the anodized layer with open structures, retaining their adhesion properties. Surface analysis of anodized samples post-treated in solutions with Ce ions and H_2O_2, prior and after corrosion tests, showed precipitation of Ce oxy-hydroxide compounds, indicating that Ce ions were incorporated in the anodic layer.[21]

One promising method to protect the exposed metal surface is to use eco-friendly alternative corrosion inhibitors in combination with a barrier coating system. Different combinations have been investigated.[18,22-26] Sol-gel coatings have been extensively studied as potential pretreatments not associated with toxic residues for aluminum alloys' surface preparation prior to paint. It has been demonstrated that they can be efficient alternatives for replacement of the chromate technology.[18,22] Lamaka, et al., used a layer of TiOx porous nanoparticles as reservoir for organic corrosion inhibitors and then a classical sol-gel coating as barrier protection to provide self-healing ability and long-term active protection for AA2024 (UNS A92024).[23-24] Ferreira, et al., studied a rare-earth conversion layer and a sol-gel film.[25] Rosero-Navaro, et al., presented a multilayered sol-gel coating with a cerium layer deposited between two undoped layers. They concluded that the presence of the cerium layer enhanced the corrosion resistance of the AA2024.[26]

The AA2524 was developed in 1990s by Aluminum Company of American (ALCOA) to substitute for AA2024. It is a version of AA2024 with lower and more controlled amounts of alloying elements, as well as lower amount of impurities.[27] Nowadays, AA2524 sheets are used as skin sheets in Boeing and Airbus aircrafts.[28] In this study, samples of AA2524 were anodized in a TSA bath and hydrothermally treated in a solution with Ce(III) ions for 5 min or 10 min, to introduce nanometric reservoirs of Ce inside the pores of the anodized layer. The commercial sealing procedure is performed during 20 min or 25 min, depending on the alloy. The effect of Ce(III) ions on the corrosion resistance of the AA2524 was investigated by SEM and EIS.

EXPERIMENTAL PROCEDURES

The cold-rolled AA2524 alloy was supplied by EMBRAER S.A. The chemical composition of the alloy was 4.07 wt% Cu, 1.66 wt% Mg, 0.60 wt% Mn, 0.10 wt% Zn, 0.11 wt% Fe, 0.03 wt% Ti, 0.01 wt% Si, and 0.02 wt% others.

Prior to anodizing, specimens of the AA2524 with dimensions of 4.5 cm × 5.0 cm × 0.105 cm were degreased by sonication in acetone for 10 min. Surface preparation was performed by dipping the samples in an alkaline etching solution: NaOH (40 g/L) at 40°C for 30 s and in a chromate-free commercial acid dismutting bath (Turco® Smuttgo-Henkel[†]) at room temperature for 15 s. Between each step of surface preparation, the specimens were thoroughly washed with distilled water.

Samples were then anodized in a TSA bath (40 g/L H_2SO_4 and 80 g/L $C_4H_6O_6$) at 10 V for 20 min at 37°C. After anodizing, some samples were immediately rinsed with distilled water and partially sealed for 5 min or 10 min by hydrothermal treatment in boiling deionized water (BW) containing or not 50 mM of Ce(III) ions, added as commercial $Ce(NO_3)_3$. The counter anion was selected in order not to provoke localized corrosion of Al, as nitrate is not aggressive to Al alloys. Addition of chloride ions was avoided to prevent localized corrosion by this type of ions.

A Gamry PCI4/300[†] potentiostat-frequency response analyzer system was used. EIS was performed in a classical three-electrode arrangement using 3.80 cm^2 area of the specimen as working electrode, Ag/AgCl (0.197 V_{SHE}) as reference electrode, and a platinum plate as counter electrode. EIS measurements were taken at different immersion times at room temperature, in a naturally aerated 0.1 mol/L NaCl solution, over a frequency range from 10^5 Hz to 10^{-2} Hz with 10 points per decade using an AC signal amplitude of 20 mV (rms). The monitoring of the electrochemical behavior during immersion test was performed up to 1,512 h, corresponding to 9 weeks. The tests were performed at least three times to ensure the reproducibility.

SEM characterization was performed in a field emission gun microscope FEI Quanta 650[†] at Nanotechnology National Laboratory in Campinas, using a working distance of 10 mm and high voltage of 20 kV, and a Hitachi SU8020[†] microscope at Materia Nova Research Centre in Mons, with a working distance around 10 mm and high voltage of 3 kV. Some areas were analyzed by energy dispersive x-ray spectrometry (EDS), to evaluate the presence/absence of Ce.

RESULTS

Figure 1 shows a SEM micrograph of the top surface of an unsealed TSA anodized AA2524 specimen showing an irregular morphology of the nanometric pores.

SEM micrographs of samples that were anodized and hydrothermally treated for 5 min or 10 min, either in BW or in solution with 50 mM of Ce(III) ions, are presented in Figure 2. All micrographs show interconnected pseudoboehmite lamellas

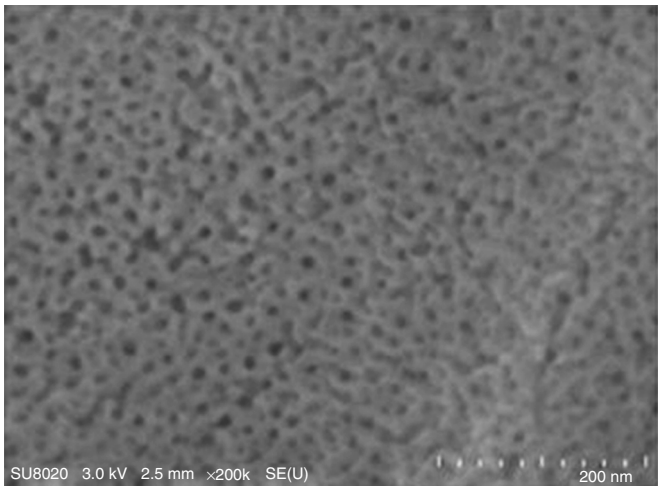

FIGURE 1. *SEM micrograph of unsealed anodized layer on AA2524.*

(1) UNS numbers are listed in *Metals and Alloys in the Unified Numbering System*, published by the Society of Automotive Engineers (SAE International) and cosponsored by ASTM International.

† Trade name.

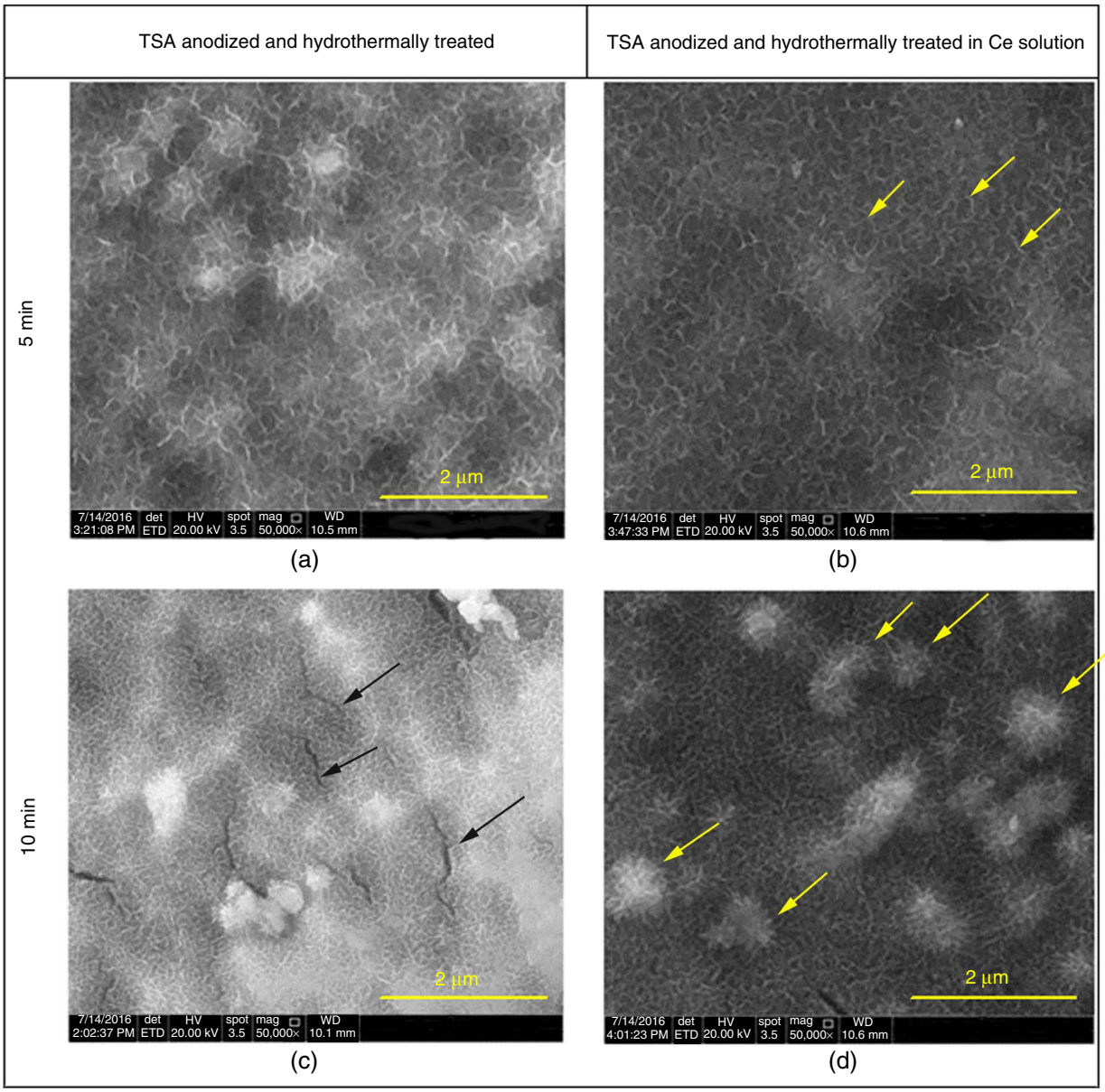

FIGURE 2. *SEM micrographs of the AA2524 TSA anodized at 10 V and hydrothermally treated in boiling water (a,b) 5 min or (c,d) 10 min, (a,c) without and (b,d) with the addition of 50 mM of Ce(III) ions.*

interlocking in various direction.[11,29] The porous nature of the anodized layer is no longer detectable in either of the samples, showing that even a short immersion period in the BW blocks the pores mouth, in accordance with the sequential mechanism proposed for pore sealing by López, et al.[11] Some cracks are clearly visible, pointed by the arrows in Figures 2(c) and (d). EDS analysis detected 2 wt% to 3 wt% of Ce at some areas of the anodized layers, mainly near the flower-shaped structures (pointed by arrows in Figure 2[d]).

EIS tests were performed up to 9 weeks to evaluate the corrosion resistance of the samples. The plots acquired in NaCl 0.1 mol/ï»¿L for samples submitted to 5 min in BW in the absence and in the presence of Ce(III) ions are depicted, respectively, in Figures 3 and 4. The same results for the samples submitted to 10 min in BW in the absence and in the presence of Ce(III) ions are depicted, respectively, in Figures 5 and 6. For most tests, the phase angle diagrams are composed of a high-frequency (HF) time constant, around 10^4 Hz, whose capacitive response varies with the immersion time and the sealing procedure, and by a wide deformed phase angle in the medium-frequency (MF), around 1 Hz, to low-frequency (LF) range, around 0.1 Hz, whose evolution is also dependent on the sealing procedure.

As shown in Figure 4(b), the addition of Ce ions to BW increases the LF impedance modulus of the anodized layer when compared to the BW sample. It remains basically above 10^6 Ω·cm^2 during the test period, and at the end of the 9 weeks exposure time it is almost two orders of magnitude higher than that exhibited by this latter sample.

Figure 5 depicts the impedance responses of a sample treated for 10 min in BW after 7 weeks test in NaCl 0.1 mol/L solution. The overall behavior was very similar to that previously described for the 5 min in BW samples: the onset of a HF time constant and an increase of the HF impedance modulus with immersion time associated with progressive pore sealing;

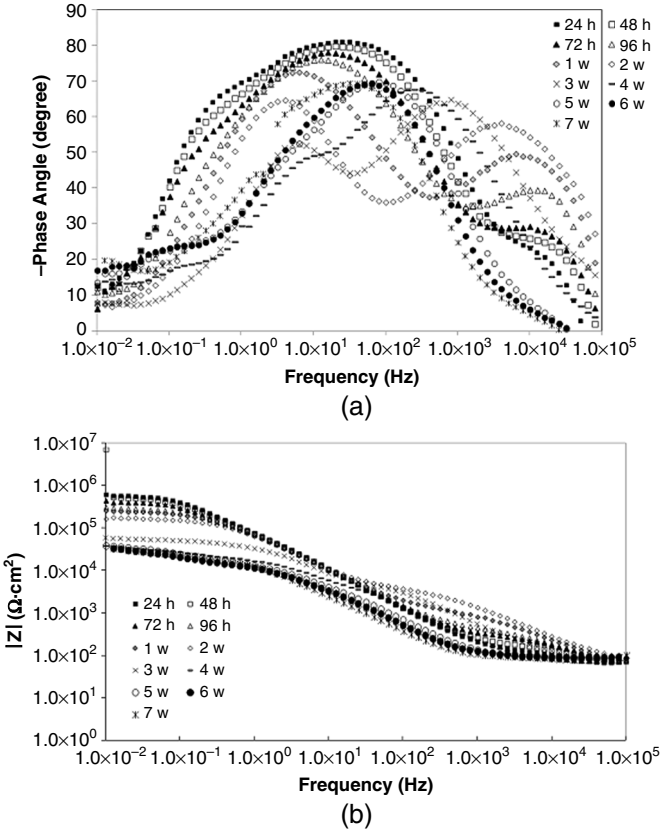

FIGURE 3. *EIS diagrams for the AA2524 TSA anodized alloy (10 V) treated for 5 min in boiling water. Immersion up to 7 weeks in a 0.1 mol/L NaCl solution. (a) Bode phase angle and (b) IZI diagrams.*

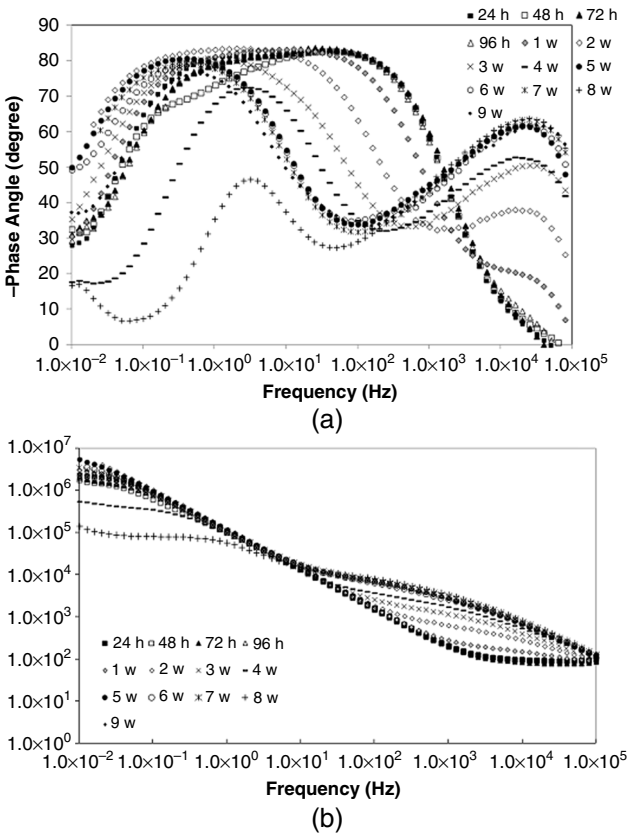

FIGURE 4. *EIS diagrams for the AA2524 TSA anodized alloy (10 V) treated for 5 min in solution with Ce (III) ions. Immersion up to 9 weeks in a 0.1 mol/L NaCl solution. (a) Bode phase angle and (b) IZI diagrams.*

better separation of the HF and LF time constants as immersion time elapses; and higher LF impedance modulus for the samples treated in Ce-containing solution. In addition, in accordance with the behavior verified for the samples treated for 5 min in Ce-containing solution, the sample treated for 10 min showed self-healing ability, which allowed the impedance modulus as well as the phase angles to recover their previous behavior after tests where impedances showed significant drops (see Figure 4[b]).

The diagrams presented in Figure 6(a) clearly show that the wide MF to LF phase angle is composed by the overlap of two time constants. This feature was already perceived in the experiments performed with the samples treated in BW for 5 min. Figure 4(a), however, was characterized only by a slight deformation of the LF phase angle for this latter condition.

Figure 7 shows the diagram representing the evolution of the impedance modulus versus time (at 0.01 Hz). The results illustrate the decrease of the impedance values with time of immersion for the BW samples and the recovery of the previous values of the BW samples in Ce solution.

Some samples were observed by SEM after 3 weeks of immersion in the NaCl 0.1 mol/L solution (Figure 8). This time of immersion was selected after the EIS tests, as some changes could be noticed in the Bode phase angle diagrams, suggesting that corrosion processes could be occurring. The micrographs showed not only localized corrosion but also corrosion products on the surface of the samples unsealed or treated in BW, pointed out by the arrows in Figures 8(a), (b), (c), and (f). On the other hand, samples treated in Ce solution presented flower-shaped structures, pointed out by the arrows in Figure 8(i), where up to 5 wt% of Ce could be detected by EDS. The cracks were only a surface feature in a few places and did not affect the corrosion resistance of the samples. Some cracked areas were covered by Ce-rich "petals," also pointed out by the arrows in Figure 8(i).

DISCUSSION

In the present work, the effectiveness of Ce(III) ion addition to a hydrothermal sealing treatment applied to 10 V TSA anodized AA2524 samples toward the anticorrosion properties of the anodized layer was investigated and tested against hydrothermally treated samples (BW).

Figure 1 presented the irregular and nanometric pores of the anodized and unsealed samples, characteristic of Al-Cu alloys. In the literature, this has been mainly ascribed not only to the rates of intermetallic particles oxidation,[30-32] but also to copper enrichment at the substrate surface, leading to incorporation of metallic or oxidized copper in the anodic film triggering oxygen generation.[33-34] However, the AA2524 is less prone to this latter phenomenon as it presents lower and more controlled alloying elements than the AA2024, as well as lower amounts of impurities, resulting in a cleaner microstructure, i.e., smaller density of intermetallics.[35]

EIS results present phase angle plots with two well-separated time constants typical of well-sealed porous anodic layer,[36-37] showing that the adopted sealing time did not lead to massive precipitation of bayerite within the pores,[11] which

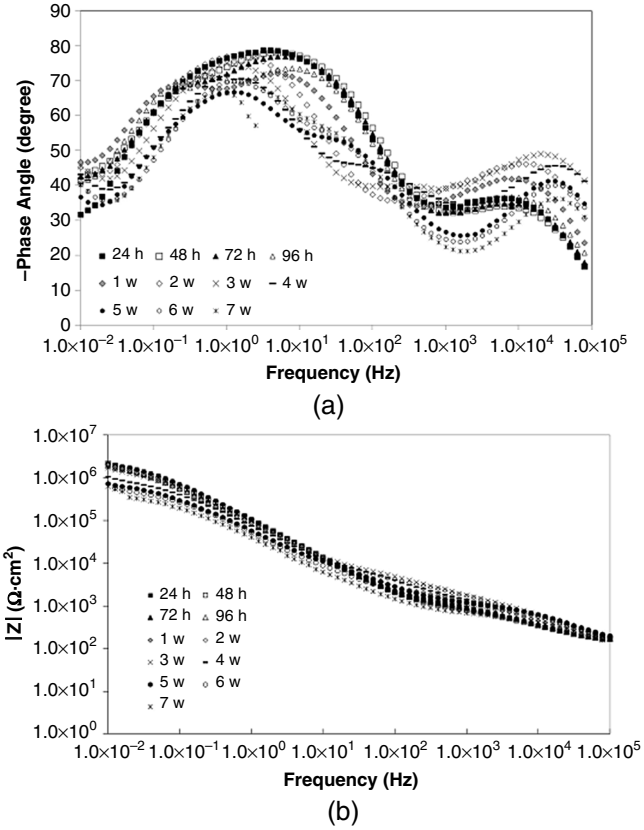

FIGURE 5. *EIS diagrams for the AA2524 TSA anodized alloy (10 V) treated for 10 min in boiling water. Immersion up to 7 weeks in a 0.1 mol/L NaCl solution. (a) Bode phase angle and (b) IZI diagrams.*

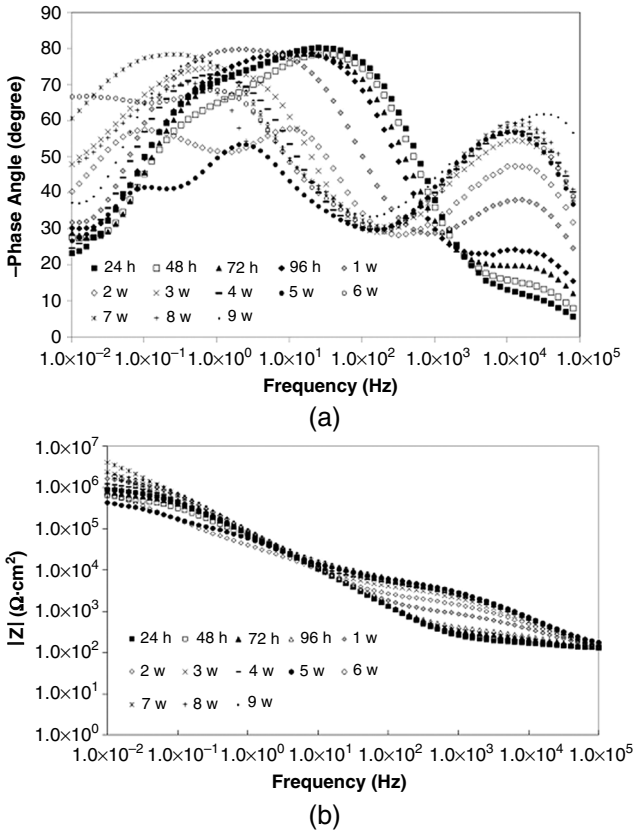

FIGURE 6. *EIS diagrams for the AA2524 TSA anodized alloy (10 V) treated for 10 min in solution with Ce(III) ions. Immersion up to 9 weeks in a 0.1 mol/L NaCl solution. (a) Bode phase angle and (b) IZI diagrams.*

could then afford superior anti-corrosion protection to the substrate. Typically, EIS results of anodized and sealed samples present two time constants due to the difference between the capacities of the barrier (very thin) and porous (thick) layers.[1,12]

The EIS results suggested that, after only one day of immersion, the LF impedance modulus of the BW samples (Figure 3[b]) is lower than 10^6 Ω·cm^2. This value is about one order of magnitude smaller than others reported in the literature for aluminum alloy substrates sealed for longer immersion times and exposed to even more aggressive solutions (3.5 wt% NaCl),[1] confirming that the sealing time adopted in the present investigation is not sufficient to effectively avoid the penetration of aggressive species through the boehmite layer into the pores. At this time, the phase angle plot is composed of a HF time constant with slightly capacitive behavior and a wide deformed MF to LF capacitive phase angle, indicating the overlap of two time constants. As immersion time increases, the impedance continuously decreases, indicating increased deterioration of the protective properties of the poorly sealed anodized layer.

As also shown in Figure 3(a), from 3 weeks of testing, the capacitive response of the HF phase angle starts to drop and is progressively shifted to lower frequencies, indicating thinning and/or contamination of the precipitated layer with ionic species. This provokes a decrease of the HF impedance modulus, pointing to easier resistive pathways through the blocked pores. At the same time, an important decrease of the LF impedance modulus and a shift of the LF phase angle to higher frequencies were verified, pointing to increased degradation of the barrier layer protective properties. From 5 weeks of testing, the HF time

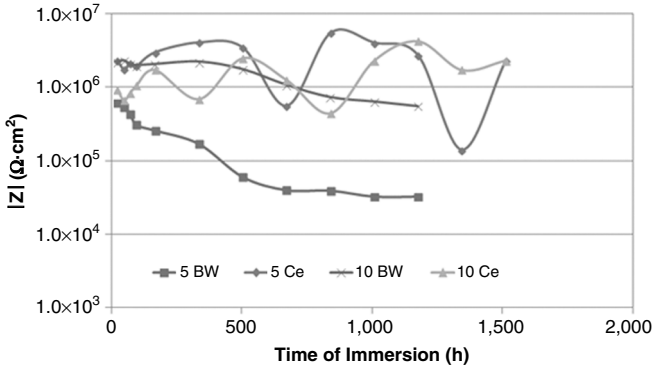

FIGURE 7. *IZI versus time of immersion in the 0.1 mol/L NaCl solution. Values obtained at 0.01 Hz.*

constant appears as just a small shoulder. At this point in the test, the LF impedance modulus has decreased by almost one order of magnitude, becoming like those presented by non-anodized Al alloys in NaCl solutions,[38-39] and another time constant is visible in the lowest-frequency region of the phase angle diagram, clearly indicating the onset of stable corrosion process at the Al/solution interface.

The data presented in Figure 3(b) also show that, up to 2 weeks of immersion, an increase of the impedance modulus in the MF region took place. This is accompanied by an increase in the capacitive response of the highest-frequency phase angle. González, et al.,[12] and Boisier, et al.,[36] investigated the effect of

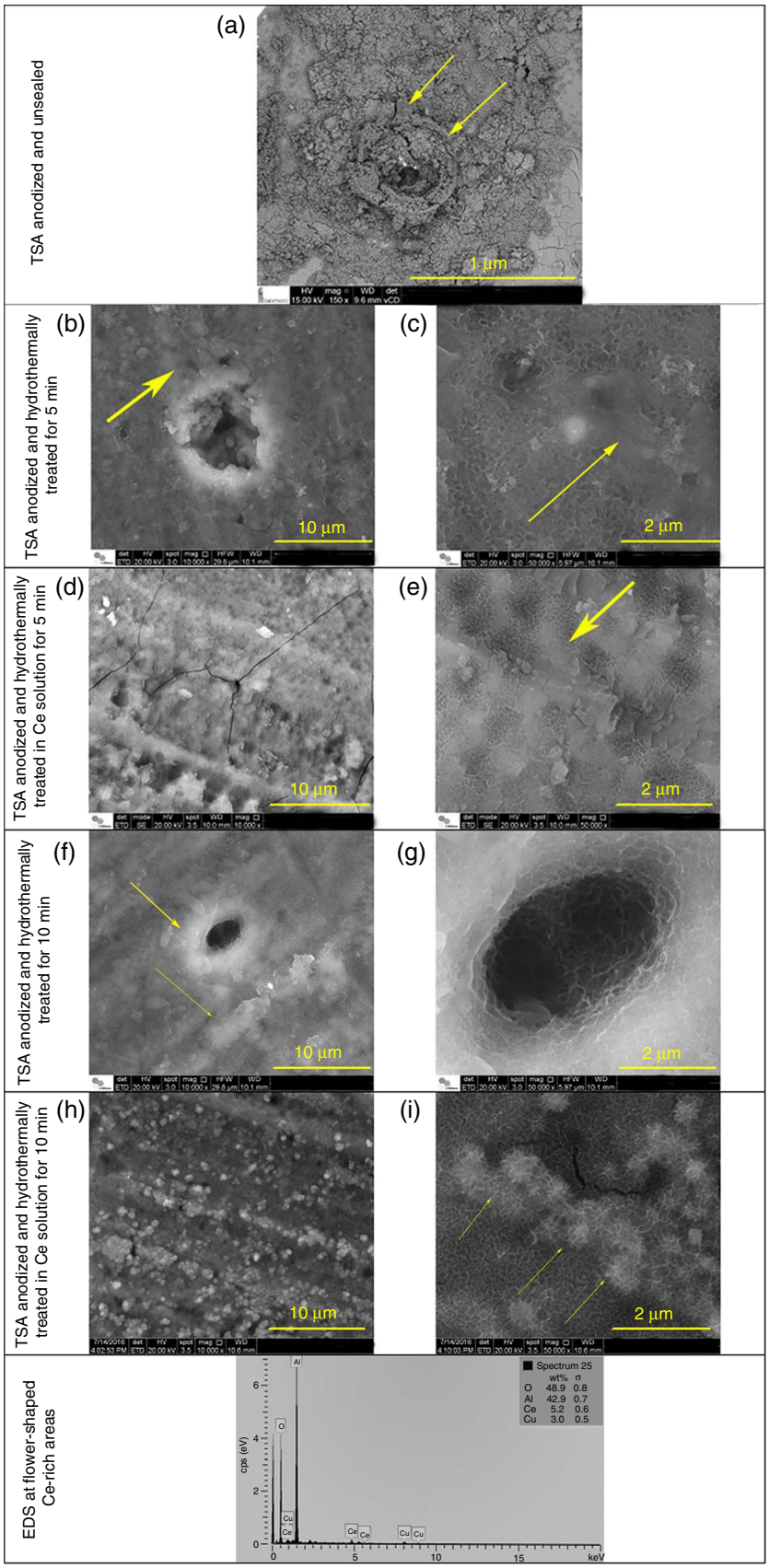

FIGURE 8. *SEM micrographs of the AA2524 TSA anodized at 10 V and hydrothermally treated in boiling water for 5 min or 10 min, with or without the addition of 50 mM of Ce(III) ions. Microstructures (b), (d), (f), and (h) are represented at higher magnifications respectively by (c), (e), (g), and (i). All samples were analyzed after 3 weeks of immersion in the 0.1 mol/L NaCl solution.*

sealing time in boiling water in the EIS response of porous aluminum anodized layer and verified that the longer the sealing time, the higher the impedance modulus in the MF range. Therefore, increased impedance modulus in this frequency range is associated with improved sealing efficient, as documented in the works of Gonzàlez, et al.,[12] and of Bosier, et al.[36] Indeed, in the experiments performed during this immersion period, the capacitive response of the highest-frequency time constant constantly increased, proving that the impedance associated with the HF process was increasing. Recently, Yang, et al.,[37] also reported the onset of a new time constant in the HF range during exposure of sealed anodized AA2024-T3 to a 3.5% NaCl solution, which was ascribed to the porous layer hydration. Therefore, the observed behavior is in accordance with literature findings, and can be ascribed to the continuation of the sealing process of the porous layer (aging by hydration) while the sample is immersed in the aggressive electrolyte. However, this does not improve the overall corrosion resistance, as the LF impedance modulus continues to slightly decrease, indicating that the precipitated bayerite inside the pores present conductive pathways through which the electrolyte and aggressive species reach the pores' bottom.

As shown in Figure 4(a), up to 96 h of testing, the sample treated with Ce(III) solution presents a wide phase angle in the MF to LF range and a small shoulder in the HF region that could be ascribed to the boehmite coverage of the pores mouth.[44] Phase angles like that found in the MF to LF range are frequently reported for porous anodized layer either unsealed or treated during short immersion times[6,12,36] and has been ascribed to unresolved time constants associated to the sealed porous layer and to the barrier layer.[12,37-44] From 1 week of immersion, the capacitive phase angle associated with the HF time constant starts to steadily increase up to the completion of the experiment (9 weeks). Meanwhile the phase angle plot starts to split in only two time constants, which progressively become better separated, and the impedance modulus in the HF to MF range starts to increase, indicating the continuation of the sealing process (aging by hydration).[12,37-44] The hypothesis of pores blocking by precipitation of corrosion products within the pores is not being considered as the main cause of the development of this HF time frequency, because when the LF impedance modulus decreases, this process is followed by a recovery of the previous impedance value, remaining relatively stable during the whole test period, indicating that there is no massive penetration of aggressive species through the treated porous layer. This indicates self-healing ability of the anodized layer, which can be likely ascribed to the presence of Ce, as reported for other protective systems.

Considering this study's impedance responses, it is proposed that the time constant at MF could be ascribed to the bayerite layer within the blocked pores. However, as aging takes place during immersion in an aggressive solution, penetration of chloride ions together with water would not allow complete pore plugging. Chloride penetration would explain both the continuous impedance modulus decrease with immersion time for the BW samples and the sudden decrease of this same quantity for the BW samples treated in Ce(III) solution. In this latter case, the self-healing ability of the plugged pore would provide the continuation of the sealing process and would explain the slight impedance increase observed for these samples.

The EIS response has shown that the BW samples treated in Ce(III) solution present a less stable behavior, particularly in the first week of immersion in the 0.1 mol/L NaCl solution, when a great decrease of impedance was verified. However, for longer test periods, EIS diagrams clearly show a recovery of the system protective properties, indicating that active protection might be imparted to the system. Figure 7 confirms the self-healing process, as the BW samples treated in Ce solution impedances at 0.01 Hz diminished, but recovered the previous value. These results are confirmed by the micrographs presented in Figure 8, where BW samples are locally corroded but those treated in Ce(III) solution showed flower- and petal-shaped structures, rich in Ce.

Certain microstructures show multiple peaks in the complex plane, which may be misinterpreted as separate electrochemical processes in real impedance data.

CONCLUSIONS

➢ In this study, samples of the AA2524 alloy were anodized in a tartaric-sulfuric acid (TSA) bath and hydrothermally treated, either in boiling water or in a solution with Ce(III) ions, for 5 min or 10 min. The hydrothermal treatments did not result in complete sealing of the anodized layer, as expected. After 3 weeks of testing, localized corrosion spots were seen in the samples hydrothermally treated in boiling water but no signs of corrosion were detected in those treated in Ce-containing solution. Also, at this test time, the impedance of the samples treated solution with Ce ions started to increase, indicating a self-healing process. The results of this work showed that Ce is in fact introduced into the pores of the anodized layer of Al alloys by hydrothermal treatment and provide long-term protection being a potential treatment for replacing post-treatments of anodized layers with Cr(VI) ions.

ACKNOWLEDGMENTS

Authors acknowledge CAPES, CNPq (Proc. 4007810/2013-1), and FAPESP (Proc. 2018/01096-5) for the financial support to this work. Dr. Maysa Terada (Proc. 1536157), Dr. Hellen Costenaro, and Dr. Fernanda Martins Queiroz (Proc. 2013/13235-6 and 2016/20572-7) are grateful for their grants awarded.

References

1. M.A. Arenas, A. Conde, J.J. de Damborenea, *Electrochim. Acta* 55, 1 (2010): p. 8704-8708.
2. P. Campestrini, E.P.M. Westing, J.H.W. Wit, *Electrochim. Acta* 46, 16 (2001): p. 2553-2592.
3. R.L. Twite, G.P. Bierwagen, *Prog. Org. Coat.* 33, 2 (1998): p. 91-100.
4. H.D. Johansen, C.M.A. Brett, A.J. Motheo, *Corros. Sci.* 63 (2012): p. 342-350.
5. EC Regulation No. 1907/2006 of the European Parliament and of the Council of 18 December 2006 concerning the Registration, Evaluation, Authorisation and Restriction of Chemicals (REACH), establishing a European Chemicals Agency, amending Directive 1999/45/EC and repealing Council Regulation (EEC) No 793/93 and Commission Regulation (EC) No 1488/94 as well as Council Directive 76/769/EEC and Commission Directives 91/155/EEC, 93/67/EEC, 93/105/EC and 2000/21/EC, *Official Journal of the European Union* L 396 (December 30, 2006).
6. M. García-Rubio, M.P. de Lara, P. Ocón, S. Diekhoff, M. Beneke, A. Lavía, I. García, *Electrochim. Acta* 54 (2009): p. 4789-4800.
7. M. García-Rubio, P. Ocón, A. Climent-Font, R.W. Smith, M. Curioni, G.E. Thompson, P. Skeldon, A. Lavía, I. García, *Corros. Sci.* 51 (2009): p. 2034-2042.
8. M. García-Rubio, P. Ocón, M. Curioni, G.E. Thompson, P. Skeldon, A. Lavía, I. García, *Corros. Sci.* 52 (2010): p. 2219-2227.
9. J.W. Diggle, T.C. Downie, C.W. Goulding, *Chem. Rev.* 69 (1969): p. 365-405.

10. V.R. Capelossi, M. Poelmanc, I. Reclouxa, R.P.B. Hernandez, H.G. de Melo, M.G. Oliveira, *Electrochim. Acta* 124 (2014): p. 69-79.
11. V. López, M.J. Bartolomé, E. Escudero, E. Otero, J.A. González, *J. Electrochem. Soc.* 153 (2006): p. B75.
12. J.A. González, V. Lopez, A. Bautista, E. Otero, *J. Appl. Electrochem.* 29 (1999): p. 229-238.
13. M. Zemanová, M. Chovancová, P. Fellner, K. Prekopp, *Chem. Papers* 52, 3 (1998): p. 152-155.
14. G. Yoganandan, J.N. Balaraju, C.H.C. Low, G. Qi, Z. Chen, *Surf. Coat. Technol.* 288 (2016): p. 115-125.
15. V. Inoue, V.R. Capelossi, W.I.A. Santos, M. Terada, I. Costa, "Effect of Polyethylene Glycol and Cerium (III) on the Corrosion Protection Properties of the Film Formed on the AA2524 Alloys by Hydrothermal Treatments," XIII SBPMat (João Pessoa, Brazil: SBPMat, 2014).
16. T.G. Harvey, *Corros. Eng. Sci. Technol.* 48 (2013): p. 248-269.
17. N.P. Tavandashti, M. Ghorbani, A. Shojaeia, Y. Gonzalez-Garcia, H. Terryn, J.M.C. Mol, *Prog. Org. Coat.* 99 (2016): p. 197-209.
18. T. Matsuda, N. Jadhav, K.B. Kashi, M. Jensen, A. Suryawanshi, V.J. Gelling, *Prog. Org. Coat.* 90 (2016): p. 425-430.
19. A. Uhart, J.B. Ledeuil, D. Gonbeau, J.C. Dupin, J.P. Bonino, F. Ansart, J. Esteban, *Appl. Surf. Sci.* 390 (2016): p. 751-759.
20. K.-B. Zhang, M.-M. Zhang, J.-F. Qiao, S.-L. Zhang, *J. Alloys Compd.* 692 (2017): p. 460.
21. O.M.P. Ramirez, F.M. Queiroz, M. Terada, U. Donatus, I. Costa, M.-G. Olivier, H.G. de Melo, *Surf. Interface Anal.* (2019): p. 1-16.
22. R.B. Figueira, C.J.R. Silva, E.V. Pereira, *J. Coat. Technol. Res.* 12 (2015): p. 1-35.
23. S. Lamaka, M. Zheludkevich, K. Yasakau, R. Serra, S. Poznyak, M. Ferreira, *Prog. Org. Coat.* 58 (2007): p. 127-135.
24. S.V. Lamaka, M.L. Zheludkevich, K.A. Yasakau, M.F. Montemor, P. Cecílio, M.G.S. Ferreira, *Electrochem. Commun.* 8 (2006): p. 421-428.
25. M.G.S. Ferreira, R.G. Duarte, M.F. Montemor, A.M.P. Simoes, *Electrochim. Acta* 49 (2004): p. 2927-2935.
26. N.C. Rosero-Navarro, L. Paussa, F. Andreatta, Y. Castro, A. Duran, M. Aparicio, L. Fedrizzi, *Prog. Org. Coat.* 69 (2010): p. 167-174.
27. E.A. DeBartolo, B.M. Hillberry, *Int. J. Fatigue* 23 (2001): p. S79-S86.
28. T.S. Srivatsan, D. Kolar, P. Magnusen, *Mater. Des.* 23 (2002): p. 129-139.
29. A. Kocjan, A. Dakskobler, T. Kosmac, *Int. J. Appl. Ceram. Technol.* 8 (2011): p. 848-853.
30. M.S. de Miera, M. Curioni, P. Skeldon, G.E. Thompson, *Corros. Sci.* 52 (2010): p. 2489-2497.
31. Y. Ma, X. Zhou, G.E. Thompson, M. Curioni, T. Hashimoto, P. Skeldon, P. Thomson, M. Fowles, *J. Electrochem. Soc.* 158 (2011): p. C17-C22.
32. R.D. Guminski, P.G. Sheasby, H.J. Lamb, *Trans. Inst. Metal Finish* 46 (1968): p. 44.
33. M. Curioni, M.S. Miera, P. Skeldon, G.E. Thompson, J. Ferguson, *J. Electrochem. Soc.* 155 (2008): p. C387-C395.
34. S.J. Garcia-Vergara, K. El Khazmi, P. Skeldon, G.E. Thompson, *Corros. Sci.* 48 (2006): p. 2937-2946.
35. H.C. Guadaguin, "Corrosion Resistance Study of AA2524 Anodized in Sulphuric-Tartaric Acid and Sealed with Hybrid Coatings" (Ph.D. thesis, University of São Paulo, Brazil, 2017).
36. G. Boisier, N. Pébère, C. Druez, M. Villatte, S. Suel, *J. Electrochem. Soc.* 155 (2008): p. C521-C529.
37. J. Yang, Y. Yang, A. Balaskas, M. Curioni, *J. Electrochem. Soc.* 164 (2017): p. C376-C382.
38. L.B. Coelho, D. Cossement, M.-G. Olivier, *Corros. Sci.* 130 (2018): p. 177-189.
39. D. Snihirova, S.V. Lamaka, P. Taheri, J.M.C. Mol, M.F. Montemor, *Surf. Coat. Technol.* 303 (2016): p. 342-351.
40. L.E.M. Palomino, P.H. Suegama, I.V. Aoki, Z. Pászti, H.G. de Melo, *Electrochim. Acta* 52 (2007): p. 7496-7505.
41. B. Hinton, *Corrosion* 66 (2010): p. 085001-085015.
42. E. Bravo-Anagua, I.V. Aoki, *Surf. Interface Anal.* 48 (2016): p. 809-817.
43. H. Costenaro, A. Lanzutti, Y. Paint, L. Fedrizzi, M. Terada, H.G. de Melo, M.-G. Olivier, *Surf. Coat. Technol.* 324 (2017): p. 438-450.
44. L. Domingues, J.C.S. Fernandes, M. da Cunha Belo, M.G.S. Ferreira, L. Guerra-Rosa, *Corros. Sci.* 45 (2003): p. 149-160.